



ELSEVIER

Contents lists available at ScienceDirect

Applied Radiation and Isotopes

journal homepage: www.elsevier.com/locate/apradiso

The feasibility of the polycarbonate Durolon™ as a thermal neutron dosimeter



F. Pugliesi^{a,b}, M.A. Stanojev Pereira^c, R. Pugliesi^{a,*}, M.S. Dias^a

^a Instituto de Pesquisas Energéticas e Nucleares, Centro do Reator de Pesquisas, Av. Prof. Lineu Prestes 2242, Cidade Universitária, 05508-000 São Paulo, Brazil

^b Instituto Divina Pastora, Physics Department, Rua dos Jatobás 70, Jabaquara, 04349-010 São Paulo, Brazil

^c Centro de Ciências e Tecnologias Nucleares, Instituto Superior Técnico, Universidade de Lisboa, Estrada Nacional 10, km 139.7, 2695-066 Bobadela LRS, Portugal

HIGHLIGHTS

- The feasibility of using Durolon™ polycarbonate for thermal neutron dosimetry was demonstrated.
- The procedure to evaluate the neutron dose takes about 23 min.
- Two digital systems for track counting and for light transmission readings were used.
- The present method is feasible for personal dosimetry and for area monitoring.

ARTICLE INFO

Article history:

Received 18 November 2013

Received in revised form

19 December 2013

Accepted 8 January 2014

Available online 23 January 2014

Keywords:

Neutron dosimetry

Track-etch detectors

Thermal neutrons

ABSTRACT

The feasibility of Durolon as a thermal neutron dosimeter was studied. As experimentally determined the proposed methodology covers a wide range of doses, from 0.1 mSv < D < 150 mSv, and can be used either for personal dosimetry or for area monitoring. Its insensitivity to visible light, beta and gamma radiations, makes the method attractive in order to evaluate neutron doses even in mixed radiation fields.

© 2014 Elsevier Ltd. All rights reserved.

1. Introduction

There is a great scientific interest in thermal neutron dosimetry, particularly in nuclear reactor facilities which are subject to mixed fields of radiation, consisting mainly of gamma-rays and neutrons. Since neutrons are not ionizing particles, they must be converted into charged particles which are able to sensitize a media, such as gas, semiconductor, scintillator, emulsion, plastic, etc., registering its passage through this media. Usually its detection is based on ${}^6\text{Li}(n, \alpha)\text{T}$ or ${}^{10}\text{B}(n, \alpha){}^7\text{Li}$ nuclear reactions, and among the commonly used neutron detectors, are those based on BF-3 and He-3 gases, thermo-luminescent, scintillators and the Solid State Nuclear Track Detectors—SSNTD, the latter employed in the present paper (Durrani and Bull, 1987; Fleisher, 1998; Ilic et al., 2003). The SSNTD's were discovered by D.A. Young in 1958, who

observed that fragments from uranium fission passing through dielectric solids such as lithium fluoride crystals leave a narrow and permanent trail of damages with diameter of about 100 Angstroms and length close to the particle range in the crystal. In 1959 Silk and Barnes have observed similar damages in mica crystals (Silk and Barnes, 1959). In 1960, Fleisher et al. (1975), Durrani and Ilic (1997), Nikezic and Yu (2004) verified that under an adequate chemical etching these damaged regions, being more reactive than the surrounding undamaged areas, are enlarged and form permanent tracks. The SSNTD are widely used in different branches of science such as in micro-pore membrane technology, nuclear physics, dosimetry, radiography and earth sciences (Rodrigues et al., 2013; Yu and Nikezic, 2011; Fleisher, 1998; Ilic et al., 2003; Szydłowski et al., 2013; Pereira et al., 2013). For thermal neutron dosimetry purposes, they exhibit several desirable properties such as insensitivity to gamma-rays, electrons and visible light, non toxicity, relatively low sensitivity for fast neutrons when compared to the one for charged particles, response to a wide thermal neutron fluence range, easy manipulation, the tracks are

* Corresponding author.

E-mail address: pugliesi@ipen.br (R. Pugliesi).

permanent, low cost, the dosimeter can be designed in several shapes and have reduced dimensions (Piesch and Burgkhardt, 1985; Vilela, 1996). Until 2008, two methods have been employed in IPEN-CNEN/SP in order to evaluate the neutron doses in SSNTD. In the first one, the track images were enlarged $1500\times$ in a microscope and they were visually counted on a video monitor screen covering an area of $1.37\times 10^{-4}\text{ cm}^2$. The time spent was about 1.5 h of uninterrupted work. In the second method, the detectors were positioned in a standard microphotometer and light transmission readings were performed through the damaged regions, by scanning several areas along the detector, each one having $2.1\times 10^{-5}\text{ cm}^2$. The time spent was about 20 min of an uninterrupted work. From 2008 and 2009, two automated digital systems were implemented in IPEN; the first for counting tracks and the second for light transmission readings. In both systems, the time spent to perform the evaluation was reduced to a few seconds and the counting statistics were improved (Pereira et al., 2008; Pugliesi, 2008). The purpose of the present paper is to demonstrate the feasibility in using the SSNTD Duroton, together with these two digital systems, for thermal neutron dosimetry purposes. The characteristics of Duroton make the method attractive to evaluate thermal neutron doses even in mixed radiation fields.

2. Experimental

The Duroton material is a polycarbonate 500 μm thick, manufactured from Makrolon by “Policarbonatos do Brasil” which was characterized as a SSNTD (Pugliesi, 2008). It has a high electric resistivity ($> 10^{16}\ \Omega\ \text{cm}$), polished surfaces and high transparency to visible light in the non-irradiated regions (Duroton, 2013; Bayer, 1997). For the purpose of the present paper, several $15\text{ mm}\times 35\text{ mm}$ pieces of Duroton have been cut and irradiated in a thermal neutron beam produced by an experimental setup installed at the radial beam-hole (BH)# 08 of the 5 MW pool type IEA-R1 nuclear research reactor of IPEN (Pereira et al., 2013). The neutron beam characteristics at the irradiation position are shown in Table 1. Since Duroton is insensitive to direct interaction with thermal neutrons, a natural boron based converter screen was used to convert neutrons into charged particles. During irradiation the detectors and the screen are kept in close contact within an aluminum cassette, as seen in Fig. 1, in such a way, the neutrons first passed through the detectors and then they reached the boron screen. The screen is a plastic backing having an overall thickness of about 170 μm (plastic $\sim 105\ \mu\text{m}$ plus a natural boron layer of $\sim 65\ \mu\text{m}$) manufactured by Kodak-Pathé (Pugliesi et al., 1999). The damages into the detectors are induced by the $^{10}\text{B}(n, \alpha)^7\text{Li}$ nuclear reaction products (α -energy=1.47 MeV; Li-energy=0.84 MeV) having intrinsic detection efficiency close to 100% (Durrani and Bull, 1987). After irradiation, the Duroton was etched in a “PEW” solution consisting of potassium hydroxide (15 g), ethanol (40 g) and water (45 g) at a constant temperature of 70 $^{\circ}\text{C}$. During etching the detectors were immersed in a glass Becker containing 400 ml of solution, and the Becker was immersed in a heat water bath. The volume of water was about 35 l and the

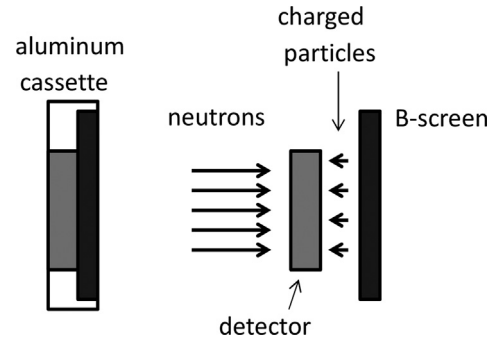


Fig. 1. Irradiation geometry: Duroton—natural boron converter screen.

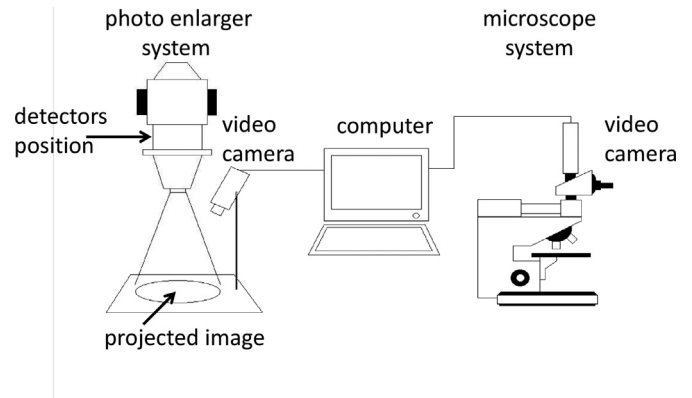


Fig. 2. Sketch of the digital systems used to evaluate the track density, and the light transmission, in the irradiated and etched detectors.

temperature gradient is minimized by water stirring. After etching, the detectors were washed in filtered water and dried by soft paper. In this stage they are ready to be analyzed in the digital systems.

The digital systems are sketched in Fig. 2. The first one, for track counting, consists of an optical microscope (Ergolux-Leitz) with a maximal magnification power of $1500\times$, coupled to a video camera. The detectors were positioned in the microscope and the magnified image of the tracks was captured by the camera and digitized by using a standard frame grabber installed in a conventional computer. After digitizing, the images were processed and the counting of tracks was automatically performed by software (Image-pro Plus V7.0). The second system used for light transmission readings, is an adapted standard photo enlarger in which a light source (75 W photo lamp) provides a divergent light beam. The detectors were positioned side by side and the light beam after passing through a set of lens impinged the detectors perpendicularly to its surface. The transmitted beam passes through another set of lens resulting in a conical divergent beam. The image of the detectors was projected on a lusterless $18\text{ cm}\times 24\text{ cm}$ white screen at a distance of 50 cm. For the present configuration the enlargement factor is about 1.5. A video camera captured the projected image which was digitized and processed by using the same computer and software previously mentioned. The light intensity was evaluated in an 8 bit gray level scale (0 to 255). In order to minimize the contribution from environmental light to the readings, the system was installed in a dark room (Pugliesi, 2008).

3. Data acquisition and results

Four parameters have been selected to demonstrate the feasibility of Duroton as a thermal neutron dosimeter.

Table 1
Characteristics of the neutron beam at the irradiation position.

Flux at the irradiation position ($\text{n cm}^{-2}\text{ s}^{-1}$)	1.75×10^6
Thermal/fast neutrons	5.7
Homogeneity (%)	~ 5
Diameter (cm)	15
Mean energy (meV)	7
Neutron dose rate (mSv s^{-1})	0.018

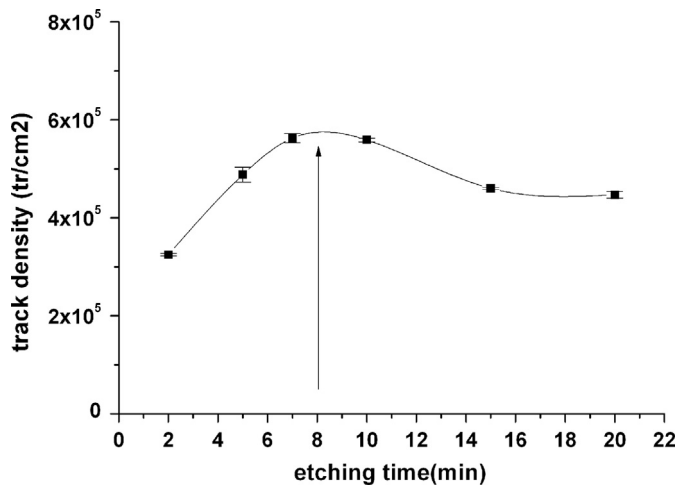


Fig. 3. Behavior of the track density as a function of the etching time.

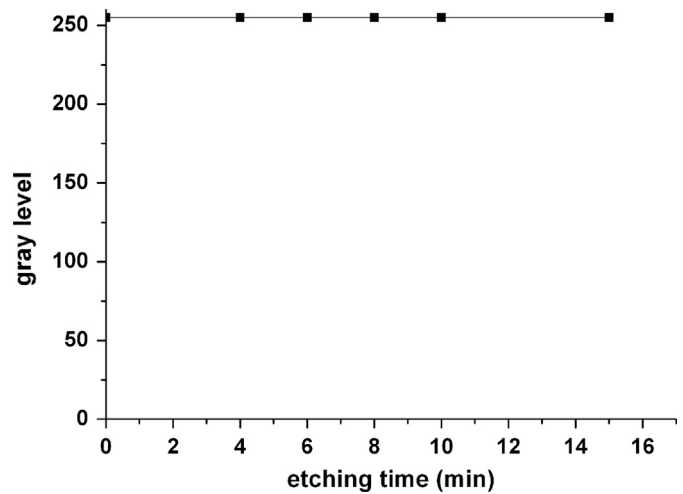


Fig. 5. Transparency of Duroton as a function of the etching time.

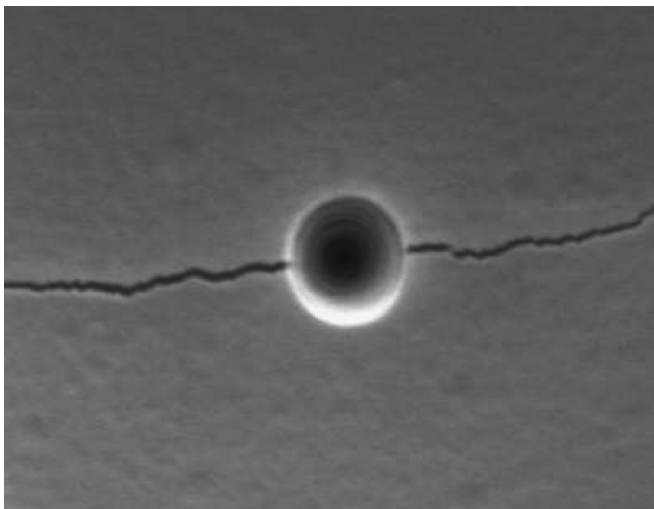


Fig. 4. Image of a track as seen in an electron microscope (20,000 ×).

3.1. Etching time

For the present, it refers to the time of etching for which the detection efficiency of Duroton is maximum. For such a purpose, six pieces of the detector have been irradiated at the same neutron fluence $3.5 \times 10^7 \text{ n cm}^{-2}$, corresponding to an irradiation of 20 s. Here, fluence (E) is defined as, $E = \phi \times t$ where “ ϕ ” is the neutron flux ($\text{n s}^{-1} \text{ cm}^{-2}$) and “ t ” is the irradiation time (s). The behavior of the track densities (track per area unit) was evaluated in the interval from 2 to 20 min of etching. For each etching time, the image was captured at a magnification of $600 \times$ and the tracks were automatically counted by the software. Fig. 3 shows the behavior of the track density as a function of the etching time. Each track density value has been determined by averaging the amount of tracks counted in 5 distinct areas of the detector, each one with $4.79 \times 10^{-4} \text{ cm}^2$, and the error bars are the standard deviation of the mean. The maximum efficiency is reached at about 8 min, and in this condition the track has a conical shape (see Fig. 4) and about $4 \mu\text{m}$ in diameter (Pugliesi, 2008).

3.2. Detector transparency as a function of the etching time

Some transparent detectors exhibit a translucent aspect after a chemical etching, leading to a decrease in the signal to noise ratio

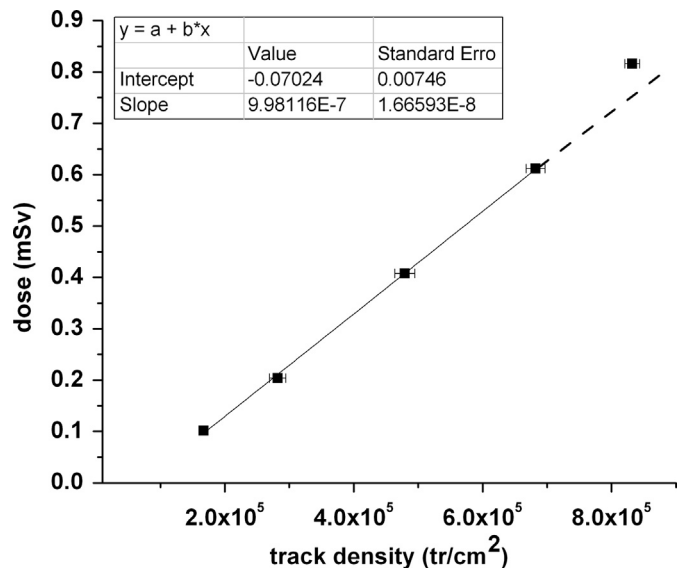


Fig. 6. Behavior of the neutron dose as a function of the track density.

(Pugliesi and Pereira, 2002; Pereira et al., 2008). For this study several pieces of non-irradiated Duroton have been etched from 0 to 15 min. The light transmission readings through the detectors were performed by using the digital system mentioned above. The behavior of transparency as a function of the etching time is shown in Fig. 5. Each gray level in the figure corresponds to an average in an area of about 0.4 cm^2 . The results show that the transparency of Duroton remains unchanged even after 15 min of etching.

3.3. Neutron dose as a function of the track production rate

For this study, five detector pieces have been irradiated in the neutron dose range $0.1 \text{ mSv} < D < 0.8 \text{ mSv}$ (American National Standard, 1977). The detectors were etched during 8 min, dried and positioned in the microscope system. The track images were captured at a magnification of $600 \times$ and the tracks were counted. Each track density value, shown in Fig. 6, has been obtained by averaging the amount of tracks counted in 5 distinct areas of the detector, each one with $4.79 \times 10^{-4} \text{ cm}^2$ and the error bars are the standard deviation of the mean. A straight line was fitted to the first four points and the result, (Eq. (1)), is

shown in Fig. 6. The interpolated doses and their uncertainties can be evaluated from the fitted parameters and by error propagation respectively. For this interval the uncertainties varies from 7% to 2.5% (Beers, 1962). For densities greater than about 7×10^5 tr cm^{-2} , the track overlapping becomes significant (Ilic and Najzer, 1990) and the linearity between, dose and track density vanishes, limiting the maximum measurable dose by track counting to ~ 0.6 mSv.

$$y = -0.07 + 9.9 \times 10^{-7} \times x \quad (1)$$

“x” is track density (tr/ cm^2) and “y” is the dose (mSv).

The reproducibility of the method was evaluated and expressed in terms of percent standard deviation, relative to the mean value of the track counting (INMETRO, 2005; Beers, 1962). The obtained value was 4.4% due to exclusively to statistics in track production, due to variation in the energy deposited by the charged particle along the damaged region, incidence angle of the particles and chemical product quality. The influence of the digital system on the reproducibility was considered to be negligible (Pugliesi, 2008).

3.4. Neutron dose as a function of the light transmission

This curve relates the neutron dose as a function of the light intensity transmitted by the irradiated and etched detectors. According to Ilic and Najzer (1990), the greater the irradiation time and the track density, the smaller the light transmission through the damaged area will be, and so, the higher the darkening in the damaged region. For such determination, about 10 detectors have been irradiated in the neutron dose range $0.2 \text{ mSv} < D < 300 \text{ mSv}$ (American National Standard, 1977). After an etching time of 8 min, the detectors were positioned in the photo enlarger system and the light transmission readings through them were evaluated. The behavior of neutron dose as a function of the gray level is shown in Fig. 7. Each gray level in the figure corresponds to an average in an area of about 0.4 cm^2 . According to these data, the method is sensitive in the $3 \text{ mSv} < D < 150 \text{ mSv}$ dose interval. For doses smaller than 3 mSv, the amount of tracks in the area is not sufficient to cause appreciable darkening of the detector, above its background. Between $3 \text{ mSv} < D < 150 \text{ mSv}$ a competition between individual track production and track overlap leads to a continuous increase of the gray level, making this region the ideal for using as a dosimeter (Ilic and Najzer, 1990). For

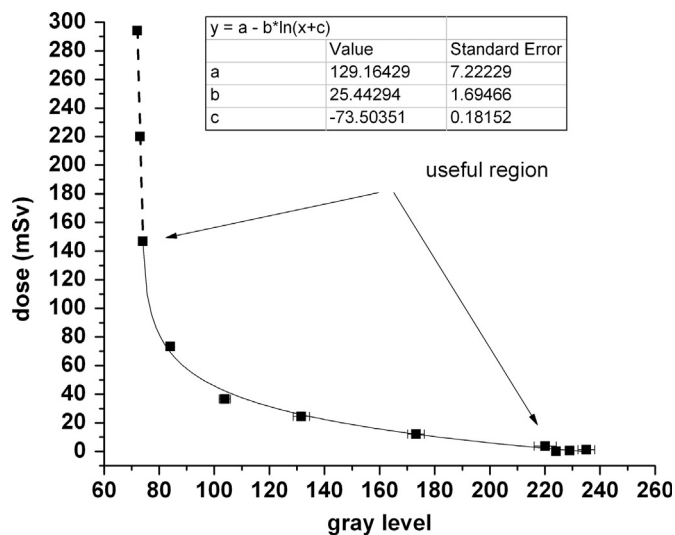


Fig. 7. Behavior of the neutron dose as a function of the gray level.

doses greater than 150 mSv the growth of the darkening is very slow, limiting the method to this maximum dose. A logarithm function (Eq. (2)) was fitted to the region of interest limited by the arrows shown in Fig. 7 and the interpolated doses and their uncertainties can be evaluated through the same procedure, as in the previous item. The resulting uncertainty for this interval ranged from 2.5% to 5% (Beers, 1962).

$$y = 129 - 25 \times \ln(x - 73) \quad (2)$$

“x” is gray level and “y” is the dose (mSv).

The reproducibility of the method was evaluated following the same procedure as in the previous item. The resulting value was 3.9% and can be attributed to statistics in the amount of tracks that cause the darkening, the energy deposited along the damaged region, angle of incidence of the particles and chemical product quality. The influence of the digital system in the reproducibility was 0.9% (Pugliesi, 2008; Pereira et al., 2008).

4. Conclusions

As experimentally demonstrated, the present methodology that makes use of the SSNTD Durodon, covers a wide range of thermal neutron doses, making it an interesting alternative for both, personal dosimetry and area monitoring.

The overall time spent to evaluate a neutron dose is about 23 min, including etching time (8 min), drying (5 min), data acquisition, processing and evaluation of the results (10 min).

It is very important to mention that due to its low efficiency for detecting fast neutrons and gamma radiation the Durodon is very useful to evaluate thermal neutron doses even in mixed radiation fields, particularly those existing in nuclear reactors.

There are at least two alternatives which can improve the present results. The first, by making use of a more adequate light transmission reader, instead of the photo enlarger, it is possible to improve the dynamic range of the reading, and so the dose limits in (Section 3.4). The second, by making use of a Boron-10 converter screen, instead natural boron, it is possible to improve the lower dose limits in both methods. Since the absorption cross section for Boron-10 is 5 times greater than the effective cross section for natural boron, more tracks are produced (NIST, 2013) and since the detector's background is the same, the greater the amount of tracks produced the better the counting statistics and the darkening of the detector.

Although the evaluated parameters have demonstrated the feasibility of Durodon as a thermal neutron dosimeter, it is necessary to study other parameters such as the energy and angular dependences for a more complete characterization.

References

- American National Standard, 1977. Neutron and Gamma-ray Flux-to-dose-rate Factors. La Grange Park, Ill: American Nuclear Society.
- Bayer AG, 1997. Application Technology Information. The Makrolon 3200 Series of Grades.
- Beers, Y., 1962. Introduction to the Theory of Error. Addison Wesley Publishing Company, Inc.
- Durodon, 2013. (<http://www.activas.com.br/downloads/especialidades/pc/IR2000.pdf>).
- Durrani, S.A.; Ilic, R., 1997. Radon Measurements by Etched Track Detectors. Applications in Radiation Protection. Earth Sciences and the Environment World Scientific, Singapore.
- Durrani, S.A., Bull, R.K., 1987. Solid State Nuclear Track Detection. Principles, Methods and Applications. International Series in Natural Philosophy, vol. 111. Pergamon Press.
- Fleisher, R.L., Price, P.B., Walker, R.M., 1975. Nuclear Tracks in Solids. Principle and Applications. University of California, Berkeley, California-U.S.A.
- Fleisher, R.L., 1998. Tracks to Innovation: Nuclear Tracks in Science and Technology. Springer.
- Ilic, R., Najzer, M., 1990. Image formation in track-etch detector-I. The large area signal transfer function. Nucl. Tracks Radiat. Meas. 17, 453–460.

- Ilic, R., Skvar, J., Golovchenko, A.N., 2003. Nuclear tracks: present and future perspectives. *Radiat. Meas.* 36, 83–88.
- INMETRO, 2005. Instituto Nacional de Metrologia, Normalização e Qualidade Industrial. Vocabulário Internacional de Termos Fundamentais e Gerais de Metrologia – VIM – 4ª edição.
- Nikezic, D., Yu, K.N., 2004. Formation and Growth of tracks in nuclear track materials. *Mater. Sci. Eng.* 46, 51–123.
- NIST, 2013. (<http://www.ncnr.nist.gov/resources/n-lengths>).
- Pereira, M.A.S., Pugliesi, R., Pugliesi, F., 2008. Neutron-induced alpha radiography. *Radiat. Meas.* 43, 1226–1230.
- Pereira, M.A.S., Schoueri, R.M., Domienikan, C., Toledo, F., Andrade, M.L.G., Pugliesi, R., 2013. The neutron tomography facility of IPEN-CNEN/SP and its potential to investigate ceramic objects from the Brazilian cultural heritage. *Appl. Radiat. Isot.* 75, 6–10.
- Piesch, E., Burgkhardt, B., 1985. *Radiat. Prot. Dosim.* 10 (1–4), 175–188 (Nuclear Technology Publishing. Albedo Neutron Dosimetry).
- Pugliesi, R., Pereira, M.A.S., Moraes, M.A.P.V., 1999. Characteristics of the solid state nuclear track detector CR-39 for neutron radiography purposes. *Appl. Radiat. Isot.* 50 (2), 375–380.
- Pugliesi, R., Pereira, M.A.S., 2002. Study of the neutron radiography characteristics for the solid state nuclear track detector Makrofol-DE. *Nucl. Instrum. Methods Phys. Res., Sect. A* 484, 613–618.
- Pugliesi, F., 2008. Characterization of Durolon as a Solid State Nuclear Track Detector. Ph.D. Thesis. Instituto de Pesquisas Energéticas e Nucleares.
- Rodrigues, G., Arruda, J.D.T., Pereira, R.M.R., Kleeb, S.R., Geraldo, L.P., Primi, M.C., Takayama, L., Rodrigues, T.E., Cavalcante, G.T., Genofre, G.C., Semmler, R., Nogueira, G.P., Fontes, E.M., 2013. Uranium deposition in bones of wistar rats associated with skeleton development. *Appl. Radiat. Isot.* 82, 105–110.
- Silk, E.C.H., Barnes, R.S., 1959. *Philos. Mag.* 4, 970.
- Szydlowski, Malinowska, A., Jaskola, M., Korman, A., Malinowski, K., Kuk, M., 2013. Calibration studies and the application of nuclear track detectors to the detection of charged particles original research. *Radiat. Meas.* 50, 258–260.
- Vilela, E.C., 1996. Development and Calibration of a Neutron Dosimeter by Using Solid State Nuclear Track Detectors. Ph.D. Thesis. Instituto de Pesquisas Energéticas e Nucleares—IPEN.
- Yu, K.N., Nikezic, D., 2011. Long-term determination of airborne radon progeny concentrations using LR 115 solid-state nuclear track detectors. *Radiat. Meas.* 46 (12), 1799–1802.